J. Innovative Eng. Nat. Sci., vol. 4, no. 2, pp. 263-275, 2024.
http://doi.org/10.61112/jiens.1396859

Journal of Innovative Engineering and Natural Science
(Yenilikçi Mühendislik ve Doğa Bilimleri Dergisi)
https://dergipark.org.tr/en/pub/jiens

Original Paper

One-step preparation of silver nanoparticle containing polymer nanocomposites via stereolithography technique

Ayberk Baykal[a], Onur Alp Aksan[a], Ahmet Yavuz Oral[b], Kaan Bilge[c,*], Nuray Kizildag[a,*]

[a]*Institute of Nanotechnology, Gebze Technical University, Kocaeli, 41400, Turkey.*
[b]*Department of Material Science and Engineering, Faculty of Engineering, Gebze Technical University, Kocaeli, 41400, Turkey.*
[c]*Insight Technology Development and Consultancy, Kozyatağı, Istanbul, Turkey.*

ARTICLE INFO

Article history:
Received 27 Nov 2023
Received in revised form 31 Jan 2024
Accepted 20 Feb 2024
Available online

Keywords:
Antibacterial
Mechanical properties
Photopolymerization
Silver nanoparticles
Stereolithography
UV-curable resins

ABSTRACT

As a technique that uses ultraviolet light to cure photo-polymers layer by layer with high spatial resolution and surface quality, stereolithography (SLA) allows for precise process control and optimization for various UV-curable polymers and their nanocomposites with various nanoparticles. In this study, UV-curable polymer nanocomposites were prepared with the addition of different contents of silver nitrate via SLA technique for use in antibacterial applications. In-situ synthesis of AgNPs was achieved during the SLA process without any additional treatments. The effect of $AgNO_3$ addition on the curing of the resin and the mechanical properties of the nanocomposite specimens were investigated. To understand the fracture mechanism of the nanocomposite samples, the fractured surfaces of the samples were evaluated by SEM, and the $AgNO_3$ content of the nanocomposite was evaluated by EDX. The nanocomposites containing 0.3 wt. % $AgNO_3$ exhibited improved mechanical properties. Further increasing the $AgNO_3$ content to 3 wt. % led to deterioration in the physical and mechanical properties of the polymer nanocomposites.

I. INTRODUCTION

Additive manufacturing (AM), defined as “the process of joining materials to make parts from 3D model data, usually layer upon layer, as opposed to subtractive manufacturing and formative manufacturing methodologies” according to ISO/ASTM 52900-15, provides a broader range of flexibilities in material design and fabrication of customized parts, fast manufacturing, waste reduction, high precision and quality at low costs in several industrial sectors, including aerospace, electronics, telecommunication, biomedical, construction, mechanical, and defence [1-4]. AM begins with a 3D model of the object, which is then digitized and sliced into model layers using a special software. The AM system then prints 2D layers into a 3D build, printing each new layer on top of the prior printed layer. Finally, a 3D object is obtained from the printer that can frequently be directly used [5]. Several technologies such as fused deposition modelling (FDM), selective laser sintering (SLS), digital light processing (DLP), and stereolithography (SLA) are available at a sufficient level of technological maturity. While FDM and SLS are the most important technologies based on processing of thermoplastic filament and powder, respectively, DLP and SLA, classified as vat photopolymerization technologies, are based on the spatially controlled solidification of a liquid resin by a fast photopolymerization reaction. With such a technique, it is possible to tailor the final properties of the printed object by simply changing the reactive formulations [6, 7]. Wider use of vat photopolymerization technologies is limited by the limited availability of commercial resins with desired mechanical and functional properties [6]. The addition of micro and nanoparticles into the polymer structure contributes to the flexibility in

*Corresponding authors. E-mail: nuraykizildag@gtu.edu.tr; kaanbilge@insighttech.info

design and fabrication of customized parts and enables the production of parts with improved structural properties and special functionalities [8, 9] and promotes the uptake of the new technologies.

The incorporation of silver nanoparticles (AgNPs) into polymers is a specific topic of interest [10]. AgNPs have attracted the interest of researchers due to their unique optical, electrical, and antibacterial capabilities, which make them promising candidates as additives in the preparation of polymer nanocomposites with functional properties. AgNPs' antibacterial properties make them effective against bacteria, viruses, and other microbes. Silver nanoparticles are also non-toxic, non-allergenic, and highly stable. Their small shape and high surface area-to-volume ratio also help to explain their increased reactivity and functionality [11-13]. UV-curable polymers, which are extensively used in additive manufacturing, can be modified by adding AgNPs so that the final printed items display antibacterial qualities [6, 14]. This is especially useful in healthcare applications, where bacterial development needs be avoided [15].

Developed in 1970s, one of the most important AM methods is SLA. It is a 3D printing method that uses ultraviolet (UV) light to solidify specific parts of a layer of photo-curable polymers. The SLA technique results in products with a high spatial resolution and low porosity [16]. It enables the in-situ synthesis of AgNPs within UV-curable resins without the need for the additional processes, which are performed for the reduction silver precursors into AgNPs in the polymer structure. The increase in the viscosity of resin after the nanoparticle addition and sedimentation of the nanoparticles in the resin limit the widespread use of the technique and call for careful selection of the resin, nanoparticle concentration and process conditions [6].

Singh and Khanna were among the first to synthesize AgNPs in poly (methyl methacrylate) (PMMA) using a one-step in-situ method. However, they initially prepared the polymer, and afterward a solution of $AgNO_3$ in DMF was added to a solution of the polymer also in DMF in order to prepare the nanocomposites material. Better thermal stability was observed when using as high as 10 wt.% of silver nitrate [17]. Using a similar approach, Singho et al. prepared PMMA/AgNPs nanocomposites and monitored the whole process using FTIR spectroscopy [18]. Siddiqui et. al. (2015) prepared nanocomposites of PMMA with AgNPs produced using an in-situ radical polymerization technique. The effect of AgNPs on the reaction kinetics was investigated by measuring the variation of conversion with time and the molecular weight distribution of the polymer formed. AgNPs with average diameter ranging from 37 to 47 nm were identified. The in-situ formation of AgNPs from the reduction of Ag^+ was explained based on a radical reaction mechanism and chain transfer reactions. It was found that the initiator efficiency was reduced by the presence of the AgNPs, resulting in a reduction of the reaction rate and a slight increase in the number average molecular weight of the polymer formed. The polydispersity as well as the glass transition temperature of the polymer was found to decrease with the amount of the AgNPs [19].

Fantino et. al. (2016) prepared 3D conductive polymeric structures by adding silver nitrate ($AgNO_3$) into a photo-curable oligomer (polyethylene glycol diacrylate (PEGDA)) in the presence of suitable photoinitiator and exposing them to the digital light system. The formulations were prepared by dissolving different amounts of $AgNO_3$ (5, 10, 15, 20 phr) in PEGDA. While the neat PEGDA matrix is an insulating material ($R > G\Omega$), the nanocomposites prepared via DLP displayed conductive properties and suggested for use in tailored applications in which charge accumulation could be detrimental (i.e., electronics) or controlled release of charge is desired [7].

Taormina et. al. (2018) demonstrated the feasibility of stereolithographic 3D printing of composite objects based on rigid photo-curable resins, containing in situ generated AgNPs from different precursors such as silver acetate,

silver acrylate, and silver methacrylate. A commercial stereolithography printer with a laser radiation was used to both cure the acrylic resin layer by layer and to reduce the silver nitrate to AgNPs. The nanocomposite samples showed improved physical and mechanical properties compared to that of the pristine matrix [6]. Valencia et al. (2022) investigated the in-situ generation of AgNPs from different Ag precursors ($AgNO_3$ and $AgClO_4$) within rigid acrylic resins via SLA. Transmission electron microscopy (TEM) analysis confirmed the formation of AgNPs smaller than 5 nm in all nanocomposites, providing optical activity to the materials. A significant reduction in the electrical resistivity up to four orders of magnitude was found for this material compared to the unfilled resin. However, consumption of part of the photoinitiator in the formation process of the AgNPs contributed to a reduction in the polymerization degree of the resin and, consequently, degraded the mechanical properties of the nanocomposites [14].

In this study, polymer nanocomposites were prepared with the addition of different contents of silver nitrate (0.3 and 3 wt.%) into tough UV-curable resin via SLA technique. The effect of $AgNO_3$ addition on the curing of the resin and the mechanical properties of the nanocomposite specimens were investigated. The most important feature of the study that distinguishes it from other studies is to obtain silver nanoparticle-reinforced nanocomposites with a desktop type SLA printer. In the future, the antibacterial properties of these nanocomposites will be investigated.

II. EXPERIMENTAL METHOD

2.1 Material

Ultracur3D® ST 80, which is a technical material based on (meth-)acrylate resin for suggested SLA systems, was used as the matrix resin. Is is colorless resin with working wavelengths of 355nm, 385 nm or 405 nm. Silver nitrate ($AgNO_3$) (Alfa Aesar Premion, 10858) was used as the precursor salt for in-situ synthesis of AgNPs in the tough photo-curable resin. Isopropanol was used in washing process.

2.2 Method

A certain amount of silver nitrate (0.3 and 3 wt.%, based on resin weight) was mixed into the resin by using a high-speed mixer at 6000 rpm for 20 minutes. The mixtures were then kept still for 10 minutes to eliminate air bubbles formed during mixing.

The CAD software Freecad was used to design the model for the specimens, the CAD file was then converted to a g-code file to be processed by the SLA printer. For composite specimen production, an Anycubic Photon Mono X 4K SLA machine was used. The neat resin and the composite resin mixtures were poured into the pool of the SLA printer. The wavelength of the UV-light was 405 nm. and the curing time for a single layer was set to 4 seconds. Each specimen consisted of 60 layers with a layer height of 5 micrometres. Neat and nanocomposite specimens were printed onto the SLA printer platform with the stacking direction along the specimen thickness in 14 minutes and used for the subsequent structural and functional characterizations. The printed specimens were detached from the printer platform and placed in Anycubic wash and cure machine for washing and post-curing processes. A 10-minute washing with ethanol was applied to remove the unreacted resin. After the washing, post-

cure was applied for 20 minutes under 405 nm UV radiation to complete the photopolymerization process. A schematic showing the printing steps via SLA technique is presented in Figure 1.

Figure 1. Schematic showing the steps followed for neat and nanocomposite specimen printing via SLA.

Four dog-bone shaped specimens and six rectangular specimens were prepared with each composition for characterization. The layout of the specimens on the printer platform is presented in Figure 2.

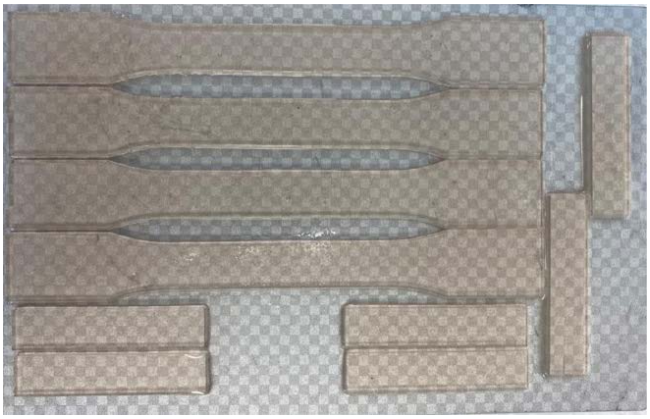

Figure 2. Layout of nanocomposite specimens on the printing bed.

2.3 Characterization

The nanocomposite samples were characterized, and their properties were compared to the neat specimens obtained in the same way without adding any silver nitrate to the resin formulation. The effect of $AgNO_3$ addition on the curing of the resin was investigated by using ultraviolet-visible spectroscopy (UV-Vis) spectroscopy and Fourier-transform infrared spectroscopy (FTIR), while the effect of $AgNO_3$ addition on the mechanical properties of the nanocomposite samples were determined by carrying out tensile tests. The surface morphology and fractured surfaces of the specimens containing different amounts of silver nitrate were analysed via scanning electron microscopy (SEM). Energy Dispersive X-ray (EDX) was used to identify and measure the elemental composition of a selected specimen. Resin mixtures were denominated with R and silver nitrate content (R-0, R-0.3, R-3), while the printed specimens were denominated with PC and silver nitrate content (PC-0, PC-0.3 and PC-3).

2.3.1. Fourier-transform infrared spectroscopy (FTIR)

Perkin Elmer FTIR Spectrometer was used to record the infra-red absorption spectra of neat and nanocomposite specimens in the range from 4000 to 700 cm^{-1} with a resolution of 4 cm^{-1}. 16 scans were taken for each specimen and averaged to produce FTIR spectra.

2.3.2. Ultraviolet-Visible spectroscopy (UV-Vis)

Shimadzu 3600i Plus Spectrophotometer was used to obtain UV-Visible spectra of neat resin and printed specimens. A scan rate of 10 nm/s was used to monitor the absorbance intensity within the wavelength range between 250 and 1000 nm.

2.3.3. Scanning Electron Microscopy (SEM)

The surface morphology and fractured surfaces of the specimens containing different amounts of silver nitrate were analysed via scanning electron microscopy. Philips XL30 SFEG scanning electron microscope was used to take SEM images. The fractured surfaces of the specimens were compared to each other.

2.3.4. The Energy Distributed X-ray (EDX) Analysis

Energy Dispersive X-ray (EDX) is a method used in the fields of analytical chemistry and materials science to identify and measure the elemental composition of given specimen. It is frequently combined with scanning electron microscopy (SEM) or transmission electron microscopy (TEM). Philips XL30 SFEG scanning electron microscope was used to take EDX images.

2.3.5. Mechanical tests

Tensile mechanical tests were performed using Instron 5569 testing machine with a load capacity of 15 kN. The samples for tensile tests were prepared and tested according to the ASTM D638 Type-I standard. The sizes of all specimens were 165 mm × 13 mm × 3 mm (length × width × thickness). Speed was set to 5 mm/min. 3 specimens were tested for each composition to determine their ultimate tensile strength.

III. RESULTS AND DISCUSSIONS

The printing process for each sample preparation lasted for 14 minutes and both the neat resin and resin mixtures were observed to be stable for the whole period without any phase separation or reaction. The printing process and the one-step preparation of nanocomposites containing AgNPs were achieved successfully. While the neat specimen was white in colour, the specimens were in brown colour and the colour became darker with the increase in the AgNPs content. The photographs of the neat and nanocomposite specimens are presented in Figure 3. The appearance of brown colour and the change in the intensity of the brown colour with the increase in the silver

nitrate content showed the formation of AgNPs during the SLA printing process without the need for any additional treatments.

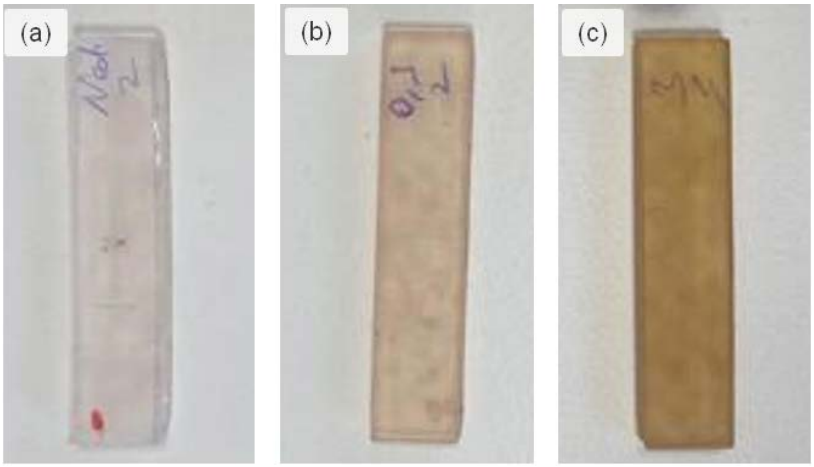

Figure 3. Photographs of the neat and nanocomposite specimens prepared via SLA. (a) PC-0, (b) PC-0.3, (c) PC-3.

3.1 Fourier-Transform Infrared Spectroscopy (FTIR)

FTIR is one of the most common methods that is used to determine the curing of photo-curable resins. The stretching vibrations of carbon-carbon double bonds involved in polymerization are detected and compared to evaluate the curing. Figure 4 shows the FTIR spectra of the printed specimens in comparison to their resins. FTIR data showed that the incorporation of AgNPs in the polymer matrix was rather physical without the formation of a strong chemical bond. In graphs it is seen that the absorption bands of acrylate group (C=C) at 1632 cm^{-1} and 812 cm^{-1} disappeared after the curing treatment as C=C bonds in the reactive monomers took part in the cross-linking reaction by photopolymerization. As the peaks disappeared completely, it is possible to say that the photopolymerization could be fully completed with the processing conditions applied.

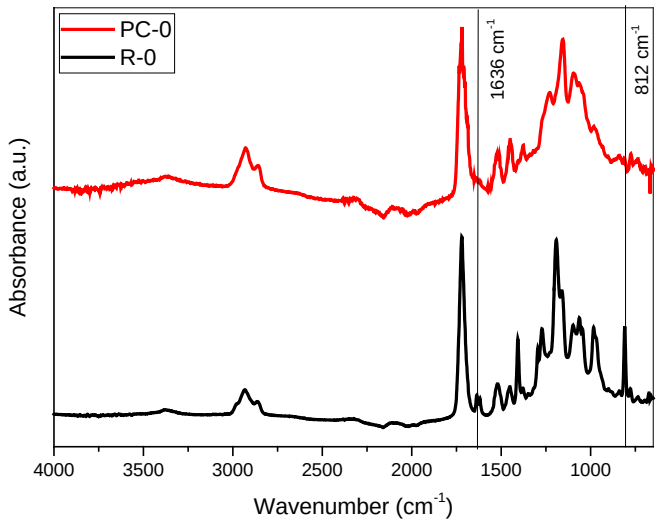

(a)

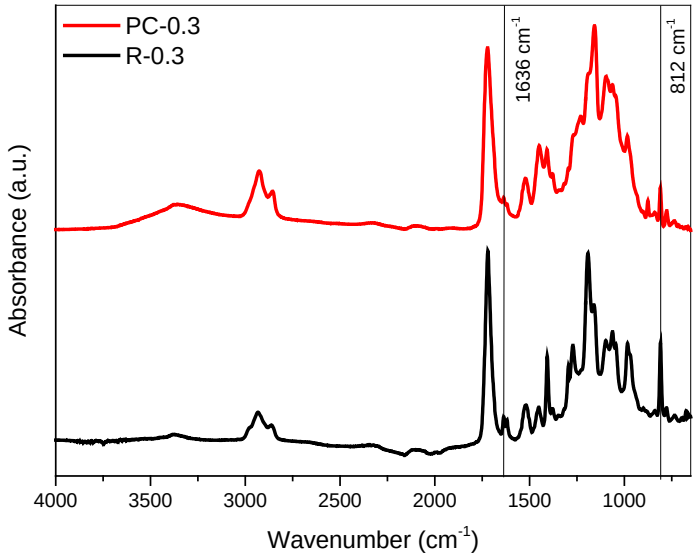

(b)

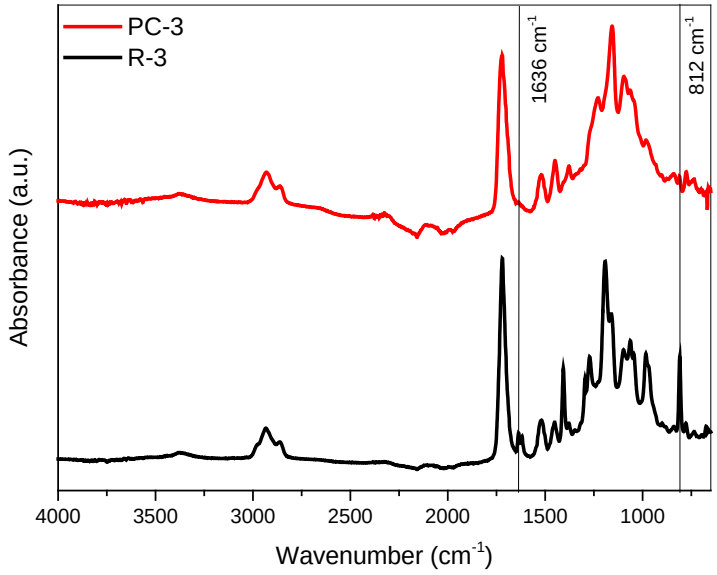

(c)

(c)

Figure 4. FTIR spectra of (a) neat resin and neat specimen, (b) resin with 3 wt.% silver nitrate and its specimen.

3.2 UV-Visible Spectroscopy

UV-Visible spectra of neat resin, neat specimen, and composite specimens with 0.3 and 3 wt.% silver nitrates are presented in Figure 5. The high absorbance of the resin between 350 and 430 nm decreased after the specimen preparation due to the photopolymerization taking place during the SLA and post-cure treatment. The lower absorbance values obtained for the composite specimens showed that the addition of silver nitrate into the resin resulted in higher monomer conversion during photopolymerization.

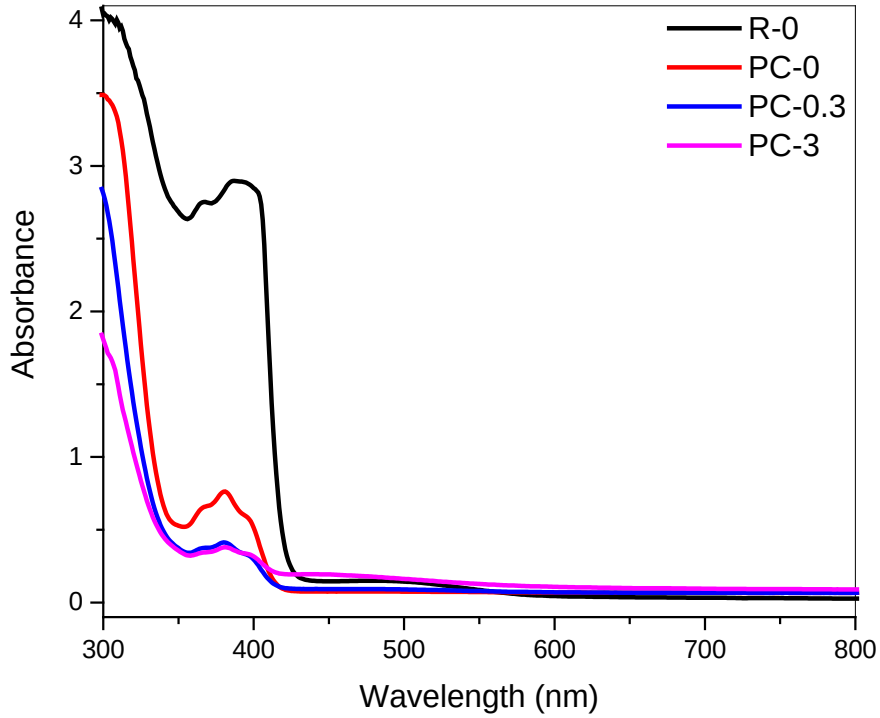

Figure 5. UV-Visible spectra of the nanocomposite specimens in comparison to neat specimen and neat resin.

3.3 Mechanical Properties and Failure

Tensile stress versus tensile strain curves obtained from performed tensile tests are shown in Figure 6. A common elastoplastic behaviour was observed both for neat and AgNPs containing samples. Measured elastic modulus values (Table 1) suggested for a significant decrease in Young's modulus for PC-3 samples. PC-0 and PC-0.3 samples had almost the same Young's modulus values. To understand such decrease in linear elastic behaviour, the repetitive building blocks obtained due to SLA technique are monitored (Figure 7). Such blocks are clearly visible on the side views of the manufactured samples (Figure 7). When PC-0 (Figure 7 (a)) and PC-0.3 samples (Figure 7(b)) are compared it can be deducted that inherently repetitive structure through the thickness morphology is preserved. Whereas for PC-3 samples (Figure7(c)) such repetition is clearly disturbed and transformed into a rather indistinctive shape. Considering the fundamental mechanism of photopolymerization in SLA, which is layer-wise, it can be claimed that the reduction in elastic modulus of PC-3 samples is due to mechanism of the photopolymerization process being affected by the silver nitrate addition.

Table 1: Tensile test results obtained from tested samples.

Sample	Elastic Modulus (MPa)	Yield Strength (MPa)	Ultimate Tensile Strength (MPa)	Strain at Failure (%)
PC-0	803.91 ± 183.60	10.77 ± 0.18	16.17 ± 0.12	9.16 ± 0.07
PC-0.3	941.17 ± 243.81	13.66 ± 2.53	17.61 ± 1.38	5.59 ± 1.46
PC-3	709.90 ± 80.26	11.04 ± 1.67	14.03 ± 2.98	5.11 ± 1.60

As the second characteristic strength parameter for elastoplastic type of resins, the yield strength values are reported in Table 1. It is clear that for PC-0.3 samples minor improvements were achieved in yield strength whereas a lower yield was measured for PC-3 samples. A similar behaviour was present for ultimate tensile strength values. The effect of silver nitrate addition is majorly visible in strain at failure values where PC-0.3 and PC-3 samples had significantly lower failure strain when compared with the neat samples.

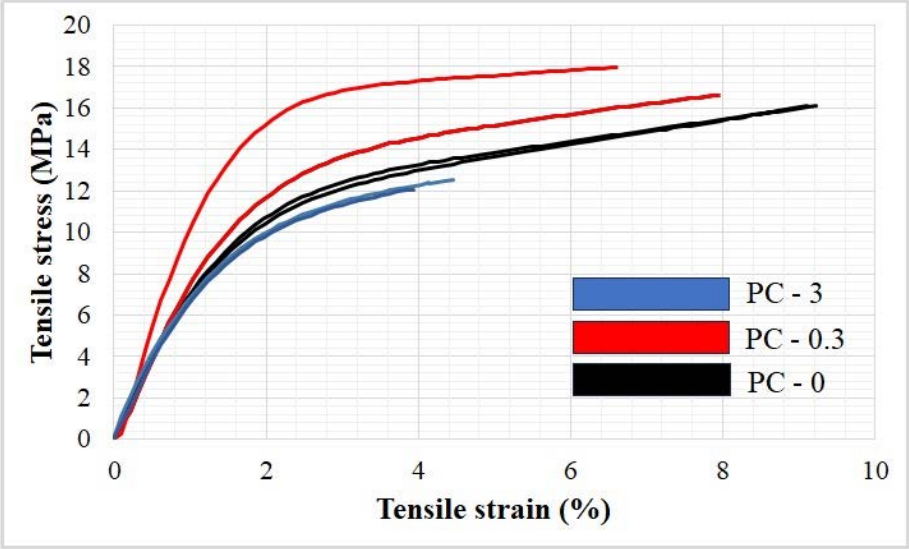

Figure 6. Representative stress-strain curves obtained from tested samples

To understand the nature of yielding and damage progression after yielding fracture surfaces of the samples were investigated. Fracture surface of neat samples is portrayed in Figure 8 (a) where oblique crack propagation (X-Y direction) towards the specimen edge is visible. This suggested that the final failure was due to shear and that the plastic hardening region after the yield point corresponds to the ability of samples to deform under shear.

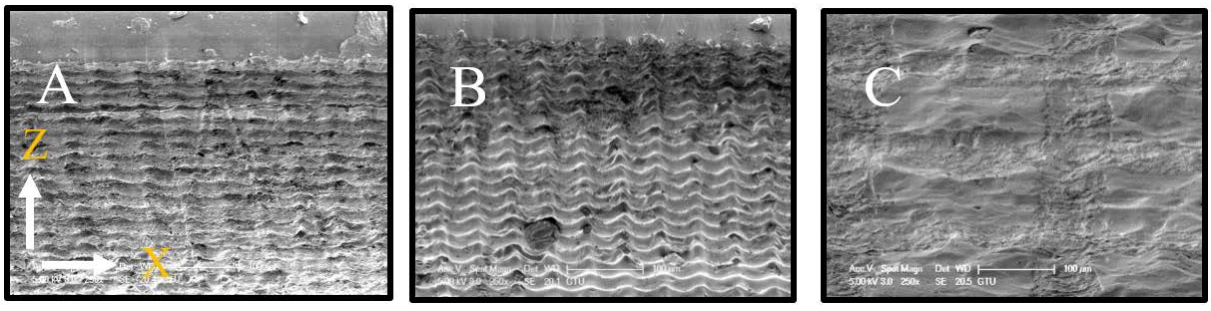

Figure 7. Cross-sectional views from a) PC-0 samples with micro building blocks visible on Z and X direction, b) PC-0.3 samples with micro-building blocks preserved, c) PC-3 samples with complete loss of building blocks.

Furthermore, it may be suggested the tensile yielding event is rather independent of the nature of building blocks in Z direction but rather dependent to repeating fashion in Y direction. A similar behaviour was observed for PC-0.3 samples (Figure 8(b)) whereas such behaviour changed to a transverse (90^0) cracking (Figure 8(c)) in the case

of PC-3. This observation clearly underlines for significant agglomerations in PC-3 samples disabling the shear deformation and enforcing an early failure (smaller strain to failure and UTS) due to transverse crack propagation during tension.

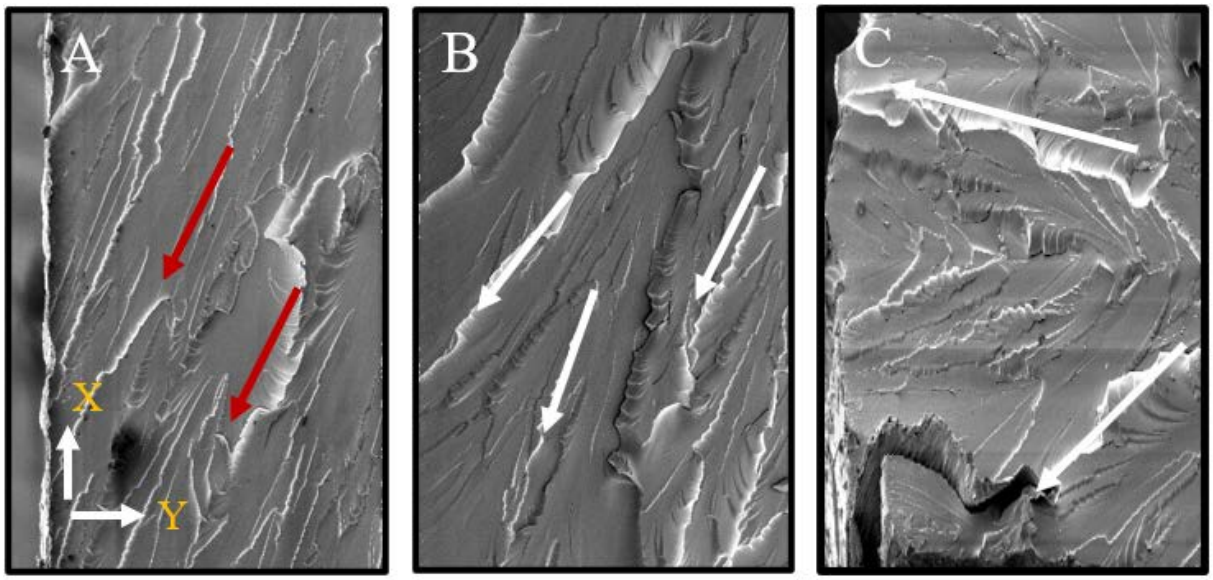

Figure 8. Tensile fracture surfaces of a) Neat sample with oblique riverlines towards the edge of the sample b) 0.3 wt% $AgNO_3$ samples with similar riverlines and ledge formation due to several micro-cracking events c) 3 wt% $AgNO_3$ samples with significant transverse cracking towards the specimens.

In overall, the tensile test results suggested that 0.3 wt.% $AgNO_3$ may be loaded into conventional UV-curing resins without deteriorating the mechanical response. For higher loading levels a better dispersion technique must be used. However, when the advantages on manufacturing time and mechanical responses are evaluated, SLA technique appears to be an effective way for implementing multifunctional $AgNO_3$ nanoparticles to conventional UV-curable resins.

3.4 The Energy Distributed X-ray (EDX)

SEM images taken from the surface of PC-0.3 sample and fractured surface of PC-3 sample are shown in Figure 8(a) and 8(c), respectively. EDX spectra showing the elemental compositions of PC-0.3 and PC-3 samples are presented in Figure 8(b) and 8(d).

SEM images of the nanocomposite samples (9(a) and (c)) showed silver particles in wide range of sizes in the polymer structure. Agglomerations were observed in silver nanocomposites but with no negative effect on mechanical strength. EDX spectra (9(b) and (d)) was acquired using spot profile mode from highly concentrated patches of AgNP on the nanocomposite SEM images (Figure 9 (a) and (c)). While no peaks related with the presence of silver were not observed for PC-0.3 sample, the EDX spectrum of PC-3 sample showed peaks of Ag atom. The visible X-ray emission line at around 3 eV corresponds to electron L shell transitions between electronic shells in silver atoms. This event releases energy in the form of X-rays as a result of electrons moving from higher energy shells to lower energy shells. The particular energy level linked to this emission, complementing the

distinctive signature of electronic transitions in the silver atoms, is unique to the elements found in the sample and provides information about its elemental composition [20]. Also, the spectrum exhibited signals originating from atoms of C, K, and N atoms, in addition to Ag atoms, which provided information about the composition of the specimen [21].

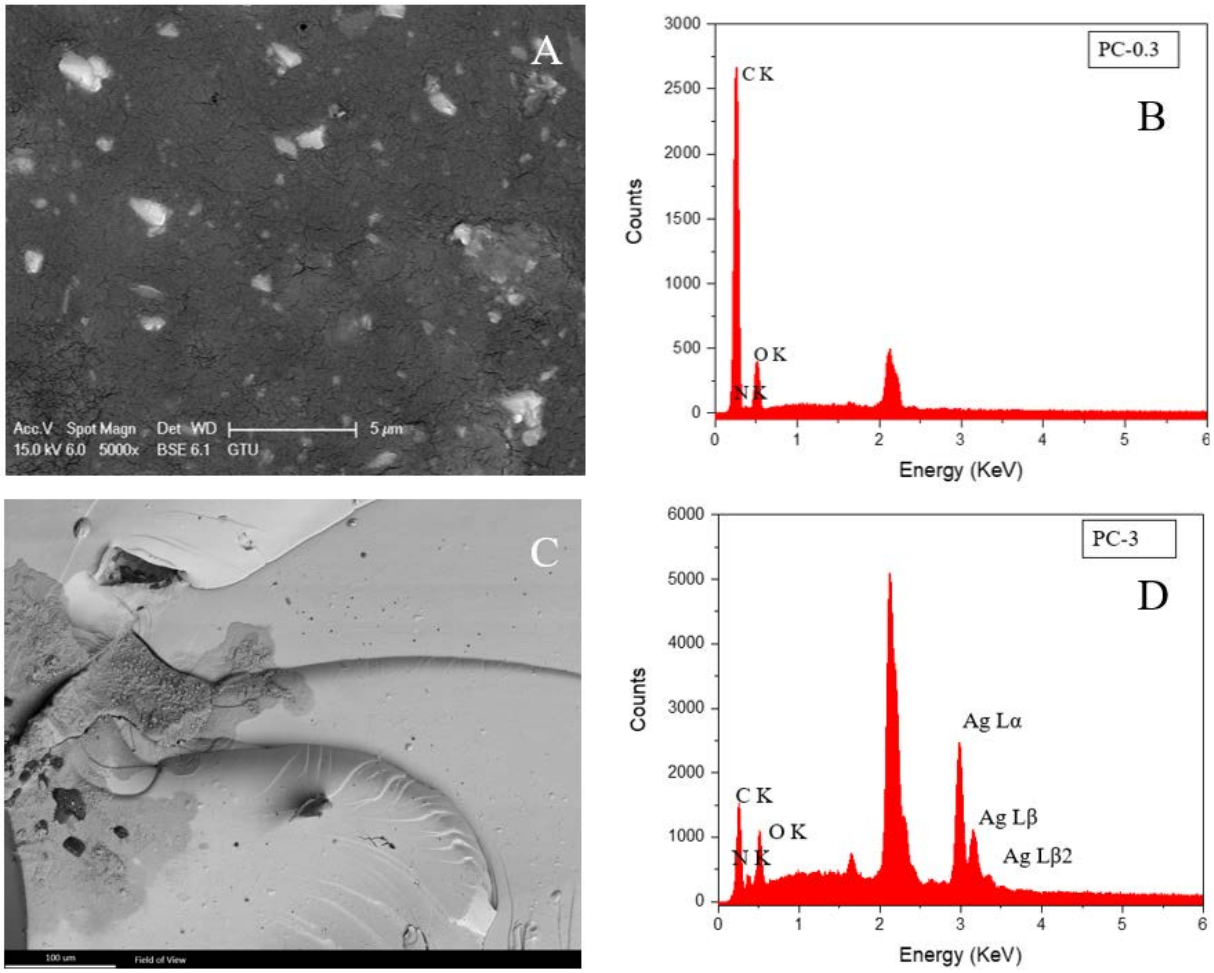

Figure 9. a) Distribution of silver particles in PC-0.3 sample b) EDX analysis of PC-0.3 samples c) Fracture Surface of PC-3 sample D) EDX analysis of PC-3 samples

EDX results of silver nanoparticles found in the article by Suresh V. Chinni et al. were observed at 3keV, similar to the results we obtained for PC-3 sample [22]. Specifically, it is hypothesized that the imbalance in EDX findings could be attributed to the formation of agglomerates during the manufacturing process. The agglomerates could have exhibited localized concentration and spatial variability during measurements.

Furthermore, the discernible and well-defined peak centered at approximately 2 keV in the X-ray spectrum is indicative of the presence of gold. This characteristic peak emanates from the gold coating applied to the sample surface, serving the dual purpose of ensuring electrical conductivity during the utilization of the scanning electron microscope (SEM) [23].

IV. CONCLUSIONS

In this study, AgNPs containing nanocomposites were prepared via SLA technique. FTIR spectra showed that the photopolymerization was completely achieved with the applied process. UV-Visible spectra showed that the addition of silver nitrate into the resin resulted in higher monomer conversion during photopolymerization. While tensile strength was improved with the addition of 0.3 wt % silver nitrate, tensile strain suffered from the silver nitrate addition. Agglomerations, which could have suppressed the mechanical improvements, were observed in SEM images. EDX analysis confirmed the presence of silver in the specimens tested. Considering the advantages of SLA technique in preparation of nanocomposites with silver nanoparticles such as very short manufacturing time, improved mechanical properties, resins containing silver nitrate are suggested for use in nanocomposite production via SLA technique. Further analyses will be carried out to investigate the antibacterial properties of the nanocomposites containing different amounts of silver nitrate prepared via SLA technique.

ACKNOWLEDGMENT

The support of Gebze Technical University through Project 2023-A-101-15 is acknowledged.

REFERENCES

1. Al Rashid A, Khan A, Al-Ghamdi SG, Koc M (2021) Additive manufacturing of polymer nanocomposites: Needs and challenges in materials, processes, and applications. Journal of Materials Research and Technology, 14:910-941. https://doi.org/10.1016/j.jmrt.2021.07.016
2. Wu H, Fahy WP, Kim S, Kim H, Zhao N, Pilato L, Kafi A, Bateman S, Koo JH (2020) Recent developments in polymers/polymer nanocomposites for additive manufacturing. Progress in Materials Science, 111: 100638. https://doi.org/10.1016/j.pmatsci.2020.100638
3. Ahangar P, Cooke ME, Weber MH, Rosenzweig DH (2019) Current biomedical applications of 3D printing and additive manufacturing. Applied Sciences, 9:1713. https://doi.org/10.3390/APP9081713
4. Nachal N, Moses JA, Karthik P, Anandharamakrishnan C (2019) Applications of 3D printing in food processing. Food Engineering Reviews 11:123–141. https://doi.org/10.1007/S12393-019-09199-8
5. Campbell TA, Ivanova OS (2013) 3D Printing of multifunctional nanocomposites. Nano Today, 8:119–120, https://doi.org/10.1016/j.nantod.2012.12.002
6. Taormina G, Sciancalpore C, Messori M, Bondioli F (2018) Advanced resins for stereolithography: In situ generation of silver nanoparticles. AIP Conference Proceedings, 1981:20065. https://doi.org/10.1063/1.5045927
7. Fantino E, Chiappone A, Roppolo I, Manfredi D, Bongiovanni R, Pirri CF, Calignano F (2016) 3D Printing of conductive complex structures with in situ generation of silver nanoparticles. Advanced Materials, 28(19):3712–3717. https://doi.org/10.1002/ADMA.201505109
8. Kartal I., Ozcan Z. (2023) Investigation of effect of chestnut sawdust on mechanical properties of epoxy matrix composites. Journal of Innovative Engineering and Natural Science, 3(2):67-74. https://doi.org/10.29228/JIENS.69363
9. Khalid MY, Imran R, Arif ZU, Akram N, Arshad H, Al Rashid A, Márquez FPG (2021) Developments in chemical treatments, manufacturing techniques and potential applications of natural-fibers-basedb biodegradable composites. Coatings, 11:293. https://doi.org/10.3390/COATINGS11030293
10. Billings C (2023) Additive manufacturing and synthesis of advanced antibacterial and sensing photocurable polymer nanocomposites. Dissertation, University of Oklahoma.
11. Sangermano M, Tagci Y, Rizza G (2007). In situ synthesis of silver-epoxy nanocomposites by photoinduced electron transfer and cationic polymerization processes. Macromolecules, 40:8827-8829. https://doi.org/10.1021/ma702051g
12. Peerzada M, Abbasi S, Lau KT, Hameed N (2020). Additive manufacturing of epoxy resins: Materials, methods, and latest trends. Industrial&Engineering Chemistry Research, 59(14):6375-6390. https://doi.org/10.1021/acs.iecr.9b06870
13. Bruna T, Maldonado-Bravo F, Jara P, Caro N (2021) Silver nanoparticles and their antibacterial applications.

International Journal of Molecular Sciences, 22(13):7202. https://doi.org/10.3390/ijms22137202
14. Valencia LM, Herrera M, de la Mata M, de León AS, Delgado FJ, Molina SI (2022) Synthesis of silver nanocomposites for stereolithography: in situ formation of nanoparticles. Polymers, 14(6):1168. https://doi.org/10.3390/polym14061168
15. Yaragatti N, Patnaik A (2021) A review on additive manufacturing of polymers composites. Materials Today: Proceedings, 44:4150-4157. https://doi.org/10.1016/j.matpr.2020.10.490
16. Anastasio R, Peerbooms W, Cardinaels R, Van Breemen LCA (2019) Characterization of ultraviolet-cured methacrylate networks: From photopolymerization to ultimate mechanical properties. Macromolecules, 52:9220–9231. https://doi.org/10.1021/ACS.MACROMOL.9B01439
17. Singh N, Khyanna P (2007) In situ synthesis of silver nano-particles in polymethylmethacrylate. Materials Chemistry and Physics, 104 (2-3):367-372. https://doi.org/10.1016/j.matchemphys.2007.03.026
18. Darman Singho N, Akmal Che Lah N, Rafie Johan M, Ahmad R (2012) FTIR Studies on silver-poly(methylmethacrylate) nanocomposites via in-situ polymerization technique. International Journal of Electrochemical Science, 7(6):5596-5603. https://doi.org/10.1016/S1452-3981(23)19646-5
19. Siddiqui MN, Redhwi HH, Vakalopoulou E, Tsagkalias I, Ioannidou MD, Achilias DS (2015) Synthesis, characterization and reaction kinetics of PMMA/silver nanocomposites prepared via in situ radical polymerization. European Polymer Journal, 72:256–269. https://doi.org/10.1016/j.eurpolymj.2015.09.019
20. Russ, J. C. (1984) Fundamentals of Energy Dispersive X-ray Analysis, Butterworths, London.
21. https://www.edax.com/resources/posters/periodic-table-poster, accessed on 29.01.2024
22. Chinni, S. V., Gopinath, S. C., Anbu, P., Fuloria, N. K., Fuloria, S., Mariappan, P., ... & Samuggam, S. (2021). Characterization and antibacterial response of silver nanoparticles biosynthesized using an ethanolic extract of Coccinia indica leaves. Crystals, 11(2), 97. https://doi.org/10.3390/cryst11020097
23. Shaban, M., Ahmed, A., Abdel-Rahman, E., Hamdy, H. (2017) Tunability and Sensing Properties of Plasmonic/1D Photonic Crystal. Scientific Reports, 7, 41983. https://doi.org/10.1038/srep41983